Journal of Thermal Analysis and Calorimetry (2024) 149:8681–8691
https://doi.org/10.1007/s10973-024-13301-6

Catalytic role of various clay minerals during the thermal reaction process with oxidized and pyrolyzed oils

Chen Luo[1] · Huiqing Liu[1] · Song Zhou[1] · Jingpeng Li[2] · Xiang Li[1] · Yaowei Huang[1]

Received: 12 March 2024 / Accepted: 19 May 2024 / Published online: 10 June 2024

Abstract

This study evaluated this thermal reaction behavior of oxidized and pyrolyzed oils containing diverse clay minerals by means of differential scanning calorimetry (DSC) technology. The catalytic role of various clay minerals for thermal reaction processes involving oxidized oil and pyrolyzed oil during in situ combustion (ISC) was investigated in conjunction with kinetic calculation methods as well. The results demonstrated that all four clay minerals could shorten its temperature region of oxidized oil low-temperature oxidation (LTO) stage, with the peak temperature during the LTO stage of oxidized oil containing montmorillonite being dramatically reduced. The catalytic role of montmorillonite and illite on oxidized oil is more powerful in the high-temperature oxidation (HTO) stage with higher peak heat flow. The Lewis acid sites within clay minerals affect free radical reactions within the crude oil pyrolysis process, and in situ reforming performance of 400°C pyrolyzed oils containing clay minerals is less effective, along with low heat release in the LTO stage. Clay minerals can considerably minimize the activation energy during thermal reaction of oxidized oil, contributing to the coke generation and conversion in the fuel deposition (FD) stage and boosting the success rate of the ISC procedure. The catalytic role of clay minerals in the oxidation and pyrolysis reactions of crude oil contributes to the prediction of fuel deposition and the expansion of the combustion front during ISC under diverse types of rock conditions.

Keywords In situ combustion · Clay mineral · Catalytic role · Oxidation · Pyrolysis · Kinetic

List of symbols

ISC	In situ combustion
LTO	Low-temperature oxidation
FD	Fuel deposition
HTO	High-temperature oxidation
α	Degree of conversion
$f(a)$	Function of the reaction model
H_t	Enthalpy released by the reaction at time t
H_o	Enthalpy released by reaction completion
t	Time
A	Arrhenius constant
T	Temperature
E	Activation energy
R	Gas constant

✉ Chen Luo
luochen_cup@163.com

✉ Huiqing Liu
Liuhq_cup@163.com

[1] State Key Laboratory of Petroleum Resources and Prospecting, China University of Petroleum, Beijing 102249, China

[2] Science and Technology on Aerospace Chemical Power Laboratory, Hubei Institute of Aerospace Chemotechnology, Xiangyang 441003, China

Introduction

In situ combustion (ISC), being highly recoverable, generated substantial heat by incinerating a portion of heavy oil in situ to activate the high-viscosity crude oil, following which crude oil mobility would be strengthened, thereby recycling the oil stored in the reservoir [1, 2]. Along with combustion proceeding in situ, the air continuously pumped into the reservoir reacted violently with heavy or ultra-thick oil, enabling the combustion front to move forward persistently; hence, the expansion and stabilization of combustion front was critical upon its success [3]. The thermal transformation properties for crude oil, inclusive of low-temperature oxidation (LTO), fuel deposition (FD), and high-temperature oxidation (HTO) of heavy oil within the oxygen atmosphere, as well as evaporation and pyrolysis of heavy oil within the inert atmosphere, beyond the field constraints, were affected

by both individual properties for crude oil itself and the atmosphere for thermal reactions [4–6]. Moreover, the clay minerals embedded in the reservoir, through their distinctive physicochemical characteristics, could also contribute substantially to heavy oil thermal conversion performance.

Clay minerals were identified as members of the layered alumino-silicates group, occurring in nature predominantly in the form of nano- to micrometer particles. Clay minerals serve as natural catalysts in rock matrices possessing high adsorption capacity, ion exchange capacity, and acid sites [7]. Vossoughi investigated the role for sand, silica, and kaolinite mixtures toward the oil combustion employing thermogravimetric (TG) and differential scanning calorimetry (DSC) methods. The process of crude oil combustion was separated into three different regions: distillation volatilization and burning/cracking procedures [8]. It was demonstrated that kaolinite could catalyze the crude oil combustion reaction [9]. Kok concluded that the crude oil oxidation peak temperature could be affected by the clay mineral fraction, whereby clay minerals catalyze crude oil LTO and HTO as well as diminish the reaction activation energy [5, 10–13]. Hascakir and Ismail demonstrated that kaolinite and illite decreased asphaltene exothermic heat of HTO, meanwhile causing an increase in asphaltene surface area and facilitating combustion reactions [14–17]. Ranjbar indicated that clay minerals of rock matrices performed a significant role in the pyrolysis reactions by increasing fuel deposition [18]. Bagci considered that the larger specific surface area of kaolinite positively influenced crude oil combustion temperatures, thereby accelerating the crude oil thermal conversion [19]. Zheng [20, 21] experimentally revealed that montmorillonite exhibited its catalytic effect on oxidized and pyrolyzed coke formation originating from Lewis and Brønsted acid sites present in the montmorillonite in accordance with the observations made by Li et al. [22, 23]. The above researches demonstrated that clay minerals, represented by montmorillonite and illite, etc., contributed to crude oil combustion, notably the oxidation and coke deposition reactions. Obviously, it was imperative for the investigation into the ISC reactions that clay minerals catalyze crude oil thermal transformations. A majority of scholars have focused on one or two clay minerals or rocks to explore the effects on crude oil thermal reforming, consisting of fuel formation, combustion front extension, and kinetic parameters. Furthermore, the studies were relatively lacking in comparing the roles by varied clay minerals upon crude oil throughout its thermal reforming stage.

Owing to the above, the effectiveness of four clay minerals on the thermal transformation characteristics within heavy oil at varied atmospheres was investigated in this work. Isothermal oxidation and isothermal pyrolysis tests were performed through mixing clay minerals separately along with quartz sand as well as heavy oil based on certain mass ratios. The catalytic role of clay minerals toward oxidized and pyrolyzed oil of variable temperatures was investigated by DSC, in comparison with that in the absence of clay minerals, revealing the influence of four species of clay minerals on the thermal reforming properties of crude oil at various atmospheres.

Experimental

Materials and preparation of sample

The laboratory crude oil provided with this research was supplied by Xinjiang Oilfield, China, with its fundamental characteristics and compositions presented by Table 1. In this work, various clay minerals were selected to investigate their catalytic roles in the thermal reaction processes for oxidized and pyrolyzed oils. The clay mineral categories tested contained montmorillonite (M), kaolinite (K), chlorite (C), and illite (I), derived from Shanghai Aladdin Biochemical Technology Co., Ltd.

Isothermal oxidized and pyrolyzed oils preparation

The experimental major equipment was the high-temperature and high-pressure-resistant customized reactor, capable of holding 600 mL of crude oil, with temperature resistance of 500 °C and pressure resistance of 40 MPa [24]. The flowchart of the experiment is illustrated in Fig. 1. The static isothermal oxidizing and isothermal pyrolyzing were employed to acquire various oxidized oils and pyrolyzed oils at different temperatures. The specific experimental process involved: Firstly, a mixture of crude oil separately with four kinds of dissimilar clay minerals and quartz sand in a 2:1:1 mass ratio, stirred uniformly, and then inserted into the reactor. Meanwhile, crude oil was homogeneously blended with quartz sand with 1:1 mass ratio which formed contrast with the previous mixtures. We set the temperature gradient of the heating furnace as 100 °C, 120 °C, and 140 °C and kept the gas pressure as 12 MPa [25]. Following the static isothermal oxidation lasting for one week, the reactor vessel was

Table 1 Fundamental characteristics and composition of crude oil

Viscosity/mPa s, 20 °C)	Components/mass%				Element/mass%				
	Saturate	Aromatic	Resin	Asphaltene	C	H	O	N	S
89,300	32.4	26.8	23.9	16.9	84.2	12.6	1.2	1.2	0.8

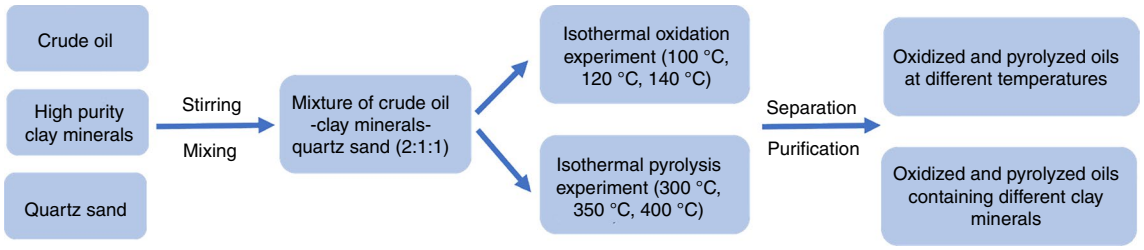

Fig. 1 Experimental flowchart

removed for obtaining 15 groups of distinct oxidized oils, and then the reactor vessel was cleaned up. Finally, in line with the previous operation, change the gas filling vessel to the inert gas with temperature gradients of 300 °C, 350 °C, and 400 °C. Again, the reactor was pyrolyzed for one week before being removed, and 15 distinct groups of pyrolyzed oils would be collected.

DSC experiments

The oxidized and pyrolyzed oils with variable temperatures were obtained through isothermal oxidizing and isothermal pyrolyzing experiments, coupled with DSC (NETZSCH DSC 214), and the catalytic function on four kinds of clay minerals toward different oxidized and pyrolyzed oils was comparatively investigated. The sample containing 5 mg (±0.5) was added, setting up the gas flow rate to 50 mL min^{-1}, while the laboratory process occurred in the air atmosphere with 99.999% purity of the air. The heating rate of the experimental procedure was 10 °C min^{-1}. A range of experimental temperatures was provided covering 30 °C–600 °C. The gas flow rate and the stabilization of the airflow were calibrated before each experiment to guarantee that the experimental error would be less than 0.1%.

Kinetic theory

Normally, non-isothermal reactions can be approximated as isothermal in miniscule time intervals, so the reactive rate for crude oil oxidizing procedure could be indicated as [26–28]:

$$\frac{\mathrm{d}\alpha}{\mathrm{d}t} = k(T)f(\alpha) \tag{1}$$

where α denotes the degree of conversion, t denotes the time, T denotes the temperature, and $f(\alpha)$ reflects a function of the reaction model. Equation (2) is the Arrhenius equation that was utilized to describe the relationship between temperature and reaction constants. The model in Eq. (3) is generally assumed to be one-level kinetics ($n=1$). The degree of conversion α in Eq. (4) is accessible by calculating from the DSC curve data.

$$k = A\exp(-E/RT) \tag{2}$$

$$f(\alpha) = (1-\alpha)^{\mathrm{n}} \tag{3}$$

$$\alpha = \frac{H_{\mathrm{t}}}{H_0} \tag{4}$$

where E denotes the activation energy, A denotes the Arrhenius constant, R denotes the gas constant, T denotes the temperature, H_{t} is the enthalpy released by the reaction at time t, and H_{o} is the enthalpy released by reaction completion. Substituting Eqs. (2), (3), and (4) into Eq. (1) yields the following equation:

$$\frac{\frac{\mathrm{d}H_{\mathrm{t}}}{\mathrm{d}t}}{H_0} = A\exp(-E/RT)\left(1-\frac{H_{\mathrm{t}}}{H_0}\right) \tag{5}$$

Equation (6) follows from the transformation, and taking logarithms on both sides gives the final Eq. (7).

$$\frac{\frac{\mathrm{d}H_{\mathrm{t}}}{\mathrm{d}t}}{H} = A\exp(-E/RT) \tag{6}$$

$$\lg\left(\frac{\frac{\mathrm{d}H_{\mathrm{t}}}{\mathrm{d}t}}{H}\right) = \lg A - E/2.303RT \tag{7}$$

Equation (7) can be used to calculate the activation energy for crude oil oxidation progress by fitting and combining the DSC data. In particular, we should pay attention to the fact that the crude oil oxidation reaction is more complex; thus, based on the Arrhenius kinetic theory, we classify the oxidation reaction processes into LTO and HTO to promote the accuracy and rigor of the calculation.

Results and discussion

Catalytic characterization of oxidized oil with diverse clay minerals

Reservoir rock matrix components constitute a critical factor in successful ISC, impacting stability and continuity along combustion leading edge [29]. It is common for the matrix containing approximately 20% assorted clay minerals, with a large specific surface area, facilitating the crude oil thermal conversion [30]. Alternatively, clay minerals possess significant catalytic effects on FD and combustion in thermal reaction processes. In the first part of this study, mixtures of 50% crude oil–25% clay minerals–25% quartz sand were prepared with four various clay minerals including montmorillonite, chlorite, kaolinite, and illite. Subsequently, the experimental samples were isothermally oxidized at varied temperatures (100 °C, 120 °C, and 140 °C) to obtain various oxidized oils. The DSC results for the oxidized oils bearing various clay minerals with heating rate of 10 °C min^{-1} and reaction temperature reaching 590 °C are shown below in Figs. 2–4.

The DSC curves in Fig. 2 showed two exothermic reaction peaks that corresponded to the reaction phases identified as LTO and HTO, respectively. A distillation reaction occurred before LTO, and partially, the 100°C oxidized oil underwent a heat absorption reaction. Table 2 provides the temperature region, peak temperature, and peak heat flow for oxidized oils containing different clay minerals in the LTO and HTO reaction phases. It would be observed for the 100°C oxidized oil that the exothermic range in the LTO region narrows down and the exothermic peak temperature lowers upon the incorporation of clay minerals. The opposite occurred in the HTO region, where 100°C oxidized oil was catalyzed by clay minerals, the HTO region expanded, and the peak heat flow rose from a maximum of 4.19–10.74 mW mg^{-1}, with the effects of illite and chlorite being more pronounced. There was a reason that the surrounding temperature was so low as well as the fact that clay minerals have a stable crystal structure that prevents them from decomposing and being transformed. Consequently, clay minerals were unable to participate in the chemical reaction except to influence the reaction rate [31].

Figure 3 shows the DSC profiles of oxidized oils at 120 °C containing different clay minerals, and the DSC images for 120°C oxidized oils without clay minerals demonstrated a three-peak distribution, which was correlated with the isothermal oxidation reaction. The major reaction processes include: evaporation of hydrocarbons,

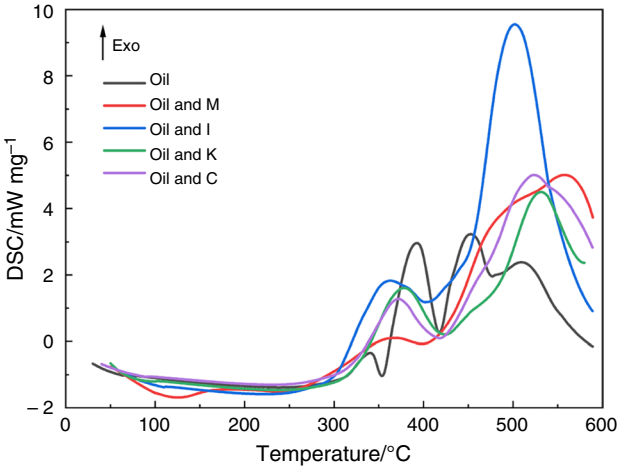

Fig. 3 DSC profiles of oxidized oil at 120 °C containing different clay minerals

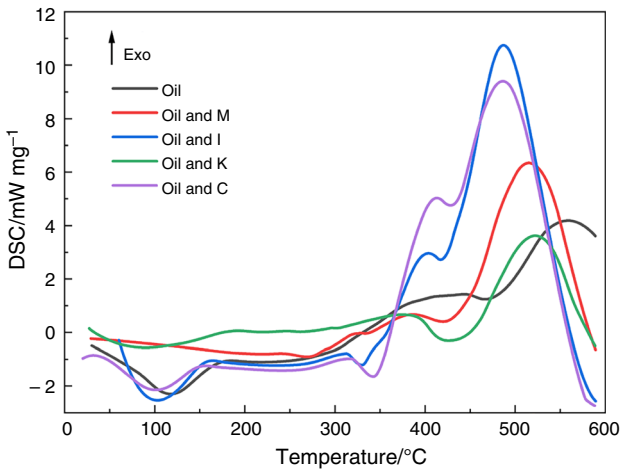

Fig. 2 DSC profiles of oxidized oil at 100 °C containing different clay minerals

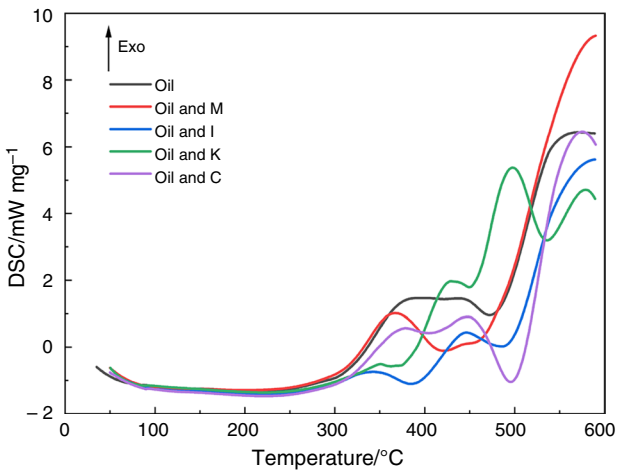

Fig. 4 DSC profiles of oxidized oil at 140 °C containing different clay minerals

Table 2 Region, peak temperature, and peak heat flow derived from DSC curves during combustion of oxidized oils containing diverse clay minerals

Sample		LTO			HTO		
		Region/°C	Peak temperature/°C	Peak heat flow/ Mw mg^{-1}	Region/°C	Peak temperature/°C	Peak heat flow/ mW mg^{-1}
100 °C	Oil	30–467	452	1.48	463–590	559	4.19
	Oil + M	30–423	386	0.67	423–590	515	6.34
	Oil + I	60–417	403	2.96	417–590	487	10.74
	Oil + K	30–427	375	0.66	427–590	524	3.62
	Oil + C	20–428	413	5.02	428–590	486	9.41
120 °C	Oil	30–417	392	2.96	417–590	453	3.23
	Oil + M	50–397	368	0.10	397–590	558	5.01
	Oil + I	60–402	362	1.83	402–590	502	9.55
	Oil + K	50–424	379	1.61	424–590	532	4.49
	Oil + C	40–418	372	1.28	418–590	523	5.01
140 °C	Oil	30–472	439	1.46	472–590	567	6.45
	Oil + M	50–421	367	1.02	421–590	589	9.03
	Oil + I	50–486	446	0.44	486–590	589	5.62
	Oil + K	50–449	429	1.97	449–590	497	5.38
	Oil + C	50–496	448	0.91	496–590	575	6.45

oxygenation reaction, isomerization, and decomposition reaction [32–34]. The FD stage tended to be accompanied by coke generation and conversion, suggesting that FD and HTO stages were integrated upon incorporation of clay minerals, and coke formation and combustion occurred concurrently [35]. The illite enlarged the peak heat flow (9.55 mW mg^{-1}) of 120°C oxidized oil at the HTO stage in comparison with other clay minerals, and the oxidized oil reacted intensely at the HTO stage (397–590 °C) to release a great deal of heat, whereas the peak temperature of 120°C oxidized oil containing clay minerals decreased in the LTO stage.

Upon raising of the isothermal oxidation temperature up to 140 °C, illustrated by Fig. 4 and Table 2, the 140°C oxidized oil became 50–421 °C within the LTO region by the catalytic role of montmorillonite, which was ascribed by the catalytic role of montmorillonite on the oxygenation reaction while catalyzing the decarbonylation and decarboxylation [36, 37]. Meanwhile, the LTO peak temperature was reduced to 367 °C, although the peak heat flow varied little; 140°C oxidized oil containing montmorillonite exhibited a greater range in the HTO region, reaching a peak temperature of 589 °C as well as peak heat flow up to 9.03 mW mg^{-1}. Incorporation of montmorillonite facilitated fuel deposition of the 140°C oxidized oil, with an earlier trigger temperature for the FD process. As the LTO process proceeded, montmorillonite selectively adsorbed on the compounds undergoing the condensation reaction, resulting in an increase in the reaction binding sites of the compounds [38, 39]. More reactive hydrogen was substituted with oxygen atoms, creating the higher-molecular-weight coke products. Moreover, an intense HTO process occurred with the increasing temperature [15, 17, 40].

Catalytic characterization of pyrolyzed oil with diverse clay minerals

In this part, isothermal pyrolysis experiments at various temperatures were conducted to obtain pyrolyzed oil at varied temperatures as well as to analyze the mechanism underlying varied clay minerals in the thermal reactions toward pyrolyzed oils. It was possible for clay minerals to convert kerogen to branched-chain hydrocarbons via the carbon ion mechanisms, as well as for the Lewis acid sites with clay minerals to drive the pyrolysis reaction through a free radical reaction. The adsorption sites with Brønsted and Lewis acids on clay minerals are schematically depicted in Fig. 5. The presence of clay minerals was considered as the cause for the decarboxylation reaction, rather than relative constitution for Lewis acidic sites, Basic sites, and Bronsted acidic sites affecting the surface active site distribution [41, 42]. The DSC profiles of pyrolyzed oil at 300 °C containing diverse clay minerals are illustrated by Fig. 6. Exothermic phenomenon began to appear as soon as the DSC test temperature reached 300 °C. There was variability in the peak heat flow and reaction interval temperature among various pyrolyzed oils upon incorporation of clay minerals. As a matter of fact, it could serve as an indication for a catalytic role of clay minerals present in the pyrolyzed oil mixtures. Table 3 demonstrates the temperature range, peak temperature, and peak heat flow of pyrolyzed oils containing diverse clay minerals during the LTO and HTO reaction phases.

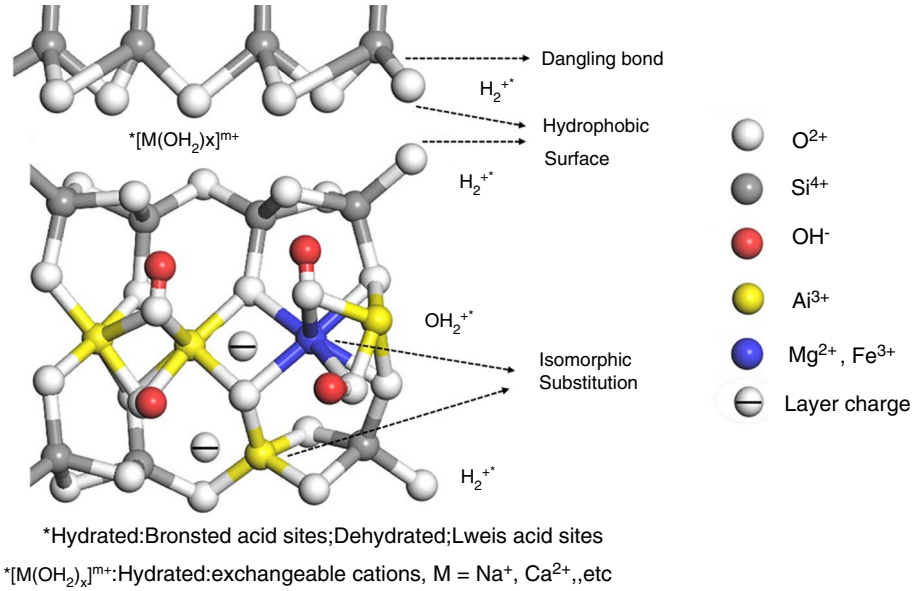

Fig. 5 Schematic representation with adsorption sites of Brønsted and Lewis acids on clay minerals [7]

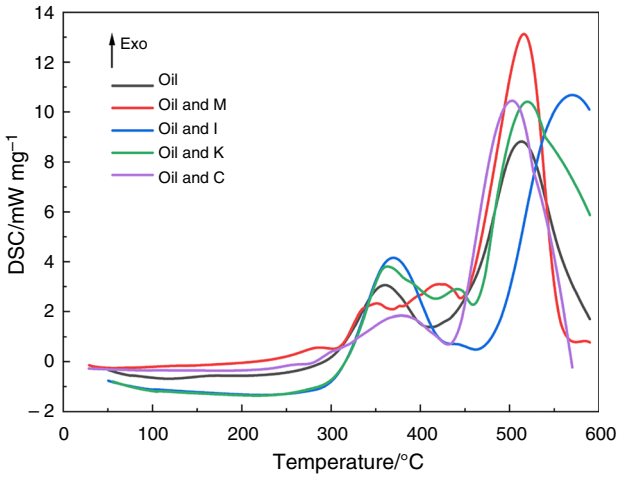

Fig. 6 DSC profiles of pyrolyzed oil at 300 °C containing different clay minerals

The peak heat flow of 300°C pyrolyzed oil containing montmorillonite reached 13.12 mW mg^{-1}, and montmorillonite showed higher catalytic activity in the HTO stage in comparison with other pyrolyzed oils. The 300°C pyrolyzed oil containing illite appeared to possess an exothermic lag with a peak temperature of 569 °C, and it might be related to the ion exchange of illite at high-temperature conditions [7, 39].

The DSC profiles of various pyrolyzed oils at 350 °C and 400 °C are illustrated by Figs. 7 and 8. Clay minerals had not modified the reaction process of 350°C pyrolyzed oil (LTO and HTO), and the catalytic effect of clay minerals was mainly manifested in the HTO stage, with montmorillonite possessing the strongest catalytic effect in the active site. Montmorillonite prolonged the reaction temperature interval of pyrolyzed oil in the LTO stage, contributing more to the generation of coke products in the FD stage. The coke products violently combusted and reacted as the reaction temperature rose, generating a large amount of heat. The peak heat flow of 350°C pyrolyzed oil containing montmorillonite was 10.01 mW mg^{-1} and 18.13 mW mg^{-1} at LTO and HTO phases, respectively. Moreover, 350°C pyrolyzed oils containing chlorite, kaolinite, and illite all exhibited a higher peak heat flow at HTO phase as compared to 350°C pyrolyzed oils without clay minerals.

Hydrocarbon cracking reaction of heavy oil was more complete with the pyrolysis temperature elevated from 350–400 °C; 400°C pyrolyzed oil had a better in situ reforming performance, and the exothermic reaction was essentially the volatilization of light hydrocarbons, resulting in a gradual decline in the amount of exothermic heat. In contrast, 400°C pyrolysis oil containing various clay minerals and exothermic reaction behaved as a gradually rising process, with the highest peak heat flow in HTO phase of the pyrolysis oil containing chlorite. Upon the pyrolysis temperature reaching 400 °C, the presence of clay minerals had an obvious retarding effect for the thermal cracking reaction of the oil, consistent here with the findings of Xiao et al. [43]. This phenomenon was associated with the water content within the crude oil, and there is variability among the clay minerals in their role within the hydrothermal cracking environments.

Kinetic analysis for oxidized and pyrolyzed oils with diverse clay minerals

In the last part of this study, we investigated further into the role of clay minerals toward the thermal transformation

Table 3 Region, peak temperature, and peak heat flow derived from DSC curves during combustion of pyrolyzed oils containing diverse clay minerals

Sample		LTO			HTO		
		Region/°C	Peak temperature/°C	Peak heat flow/ mW mg^{-1}	Region/°C	Peak temperature/°C	Peak heat flow/ mW mg^{-1}
300 °C	Oil	50–410	360	3.06	410–590	513	8.82
	Oil + M	30–445	422	3.10	445–590	516	13.12
	Oil + I	50–462	369	4.15	462–590	569	10.68
	Oil + K	50–458	363	3.80	458–590	520	10.41
	Oil + C	30–431	380	1.84	431–570	503	10.45
350 °C	Oil	50–417	356	3.67	417–590	527	8.58
	Oil + M	30–516	425	4.07	516–590	590	17.82
	Oil + I	30–442	358	2.62	442–590	513	10.93
	Oil + K	30–417	372	3.44	417–590	492	15.92
	Oil + C	30–437	382	3.66	437–590	503	17.02
400 °C	Oil + M	30–442	421	1.14	442–590	524	3.28
	Oil + I	30–447	433	1.06	447–590	532	4.31
	Oil + K	30–445	437	1.11	445–590	528	3.74
	Oil + C	30–417	359	1.22	417–590	569	4.59

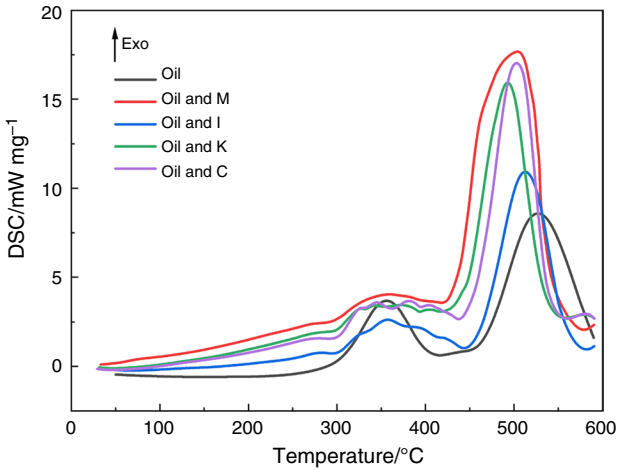

Fig. 7 DSC profiles of pyrolyzed oil at 350 °C containing different clay minerals

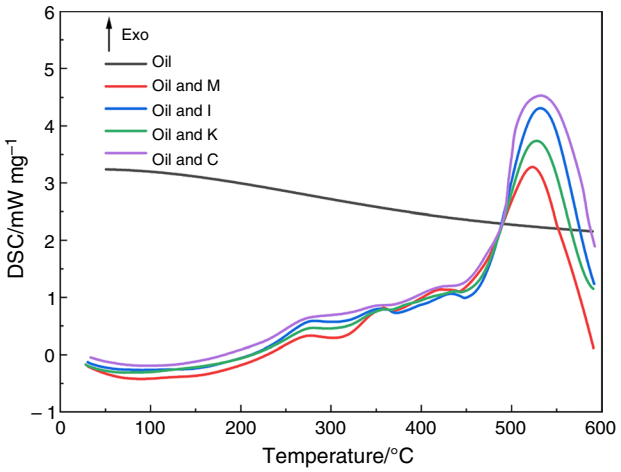

Fig. 8 DSC profiles of pyrolyzed oil at 400 °C containing different clay minerals

characteristics for oxidized and pyrolyzed oils through calculating the activation energy at distinct reaction stages via the kinetic theory depicted in Sect. "Experimental." Table 4 depicts the activation energy for oxidized oils containing diverse clay minerals at LTO and HTO phases. The activation energy of LTO increased up to 32.08 kJ mol^{-1} for pure heavy oil oxidation temperature raised to 140 °C from 100 °C. The activation energy of oxidized oil with clay minerals started to reduce gently along with rising oxidation temperature. The activation energy reduction rate of 140°C oxidized oil during LTO phase was approximately 60% (the lowest activation energy was 29.09 kJ mol^{-1}) due to the catalytic role of montmorillonite and chlorite. In the HTO stage, a weaker contribution from clay minerals to activation energy of oxidized oil was observed. The activation energy reduction percentage for oxidized oil with clay minerals rose from 22 to 34% following oxidation temperature increase. It could be recognized that the catalytic activities with clay minerals were relevant to reaction temperature, and clay minerals had the remarkable role on the activation energy of oxidized oil at the LTO stage. Overall, if the combustion front could tend to propagate steadily during ISC implementation, presentation of clay minerals could promote the LTO reaction, transition to the FD stage faster, generate more oxidized coke to support the combustion front to

Table 4 Activation energy for oxidized oils with diverse clay minerals at LTO and HTO stages

Sample		Activation energy/ kJ mol^{-1}	
		LTO	HTO
100 °C	Oil	43.77	128.64
	Oil and M	39.41	103.43
	Oil and I	39.48	106.81
	Oil and K	41.04	115.02
	Oil and C	37.73	99.56
120 °C	Oil	53.32	141.79
	Oil and M	38.54	109.58
	Oil and I	37.27	121.62
	Oil and K	40.21	119.95
	Oil and C	33.15	108.43
140 °C	Oil	75.85	218.23
	Oil and M	30.12	150.91
	Oil and I	37.04	165.72
	Oil and K	35.54	143.27
	Oil and C	29.09	152.05

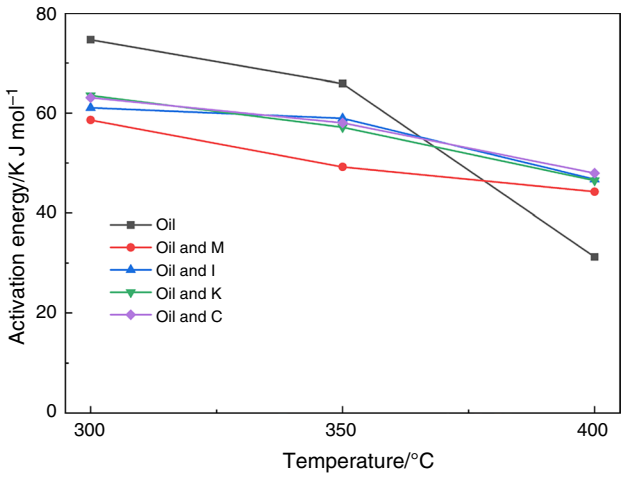

Fig. 9 Activation energy of diverse pyrolyzed oils at the LTO stage

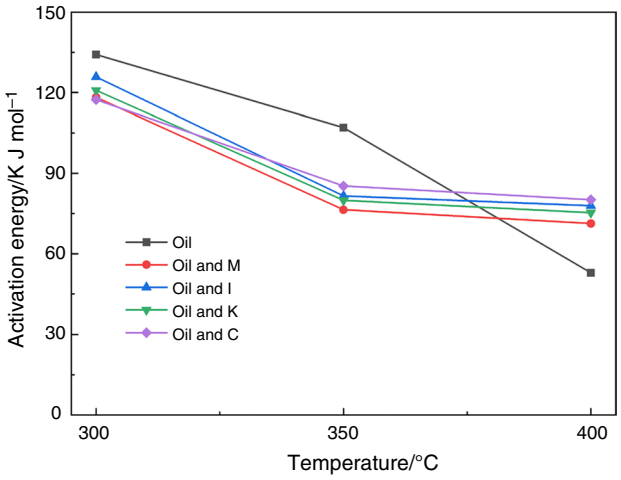

Fig. 10 Activation energy of diverse pyrolyzed oils at the HTO stage

Table 5 Activation energy for pyrolyzed oil with diverse clay minerals at LTO and HTO stages

Sample		Activation energy/ kJ mol^{-1}	
		LTO	HTO
300 °C	Oil	74.69	134.15
	Oil and M	58.62	118.23
	Oil and I	61.07	125.86
	Oil and K	63.55	120.82
	Oil and C	63.12	117.39
350 °C	Oil	65.92	106.98
	Oil and M	49.23	76.43
	Oil and I	58.97	81.59
	Oil and K	57.19	79.92
	Oil and C	58.06	85.27
400 °C	Oil	31.26	52.91
	Oil and M	44.26	71.28
	Oil and I	46.74	77.95
	Oil and K	46.52	75.33
	Oil and C	47.98	80.16

continue to move forward, and boost the success rate of the ISC procedure [36, 44, 45].

The participation by clay minerals within the pyrolysis reaction of the oil carried with itself the possibility of diagenetic reactions at high-temperature conditions, involving the transformation of kaolinite into chlorite and/or chlorite. Table 5 describes the pyrolyzed oil activation energy with diverse clay minerals at the LTO and HTO stages. The preceding Sect. "Catalytic characterization of pyrolyzed oil with diverse clay minerals" described that the chemical bonds of macromolecular hydrocarbons were broken once the pyrolysis temperature reached 400 °C, and they were completely cracked and reformed into hydrocarbons with smaller molecular weights; hence, 400°C pyrolyzed oil had the least activation energy during the LTO stage. Then, Fig. 9 reflects the activation energy corresponding to pyrolyzed oils containing diverse clay minerals during the LTO stage. Presentation of clay minerals retarded thermal cracking reaction for crude oil significantly; thus, the pyrolyzed oil without clay minerals exhibited the lowest activation energy (31.26 kJ mol^{-1}) during the LTO stage. Moreover, the strong adsorption of montmorillonite in comparison with other clay minerals manifested in adsorption of polar and heavy components in crude oil, promoting LTO

reaction process [46]. The acidic fraction generated during the cracking and reforming process of crude oil also intensified the Lewis acidic and Brønsted acidic sites of montmorillonite themselves, catalyzing the LTO process, while illite, kaolinite, and chlorite have similar catalytic activity. Activation energy of diverse pyrolyzed oils at the HTO stage is illustrated in Fig. 10. The activation energy declined when the reaction spread to HTO stage, and the range of activation energy for 400°C pyrolyzed oil was 52.91–80.16 kJ mol^{-1}. The activation energy of pyrolysis oils containing clay minerals was much higher than pure pyrolyzed oil. This effect of clay minerals in HTO on the activation energy was observed predominantly in 300°C pyrolyzed oil and 350°C pyrolyzed oil. Since the strong adsorption of clay minerals, they could adsorb and participate in the reaction with polarity fractions and heavy fractions within the oil. However, the Lewis and Brønsted acid sites existing inside clay minerals were capable of catalyzing the fracture and reorganization of long-chain hydrocarbons within the oil, whereby the oil underwent the cracking, isomerization, and transformation procedures, allowing the conversion of carbon ions into hydrocarbons [47, 48]. The conversion between clay minerals was completed after the pyrolysis temperature was sufficiently high. At the same time, the fractions within clay minerals adsorbed strongly on their hydrocarbon surfaces, causing the products to become more heat-resistant and stable; thus, the thermal conversion reaction was more difficult to take place. It could be inferred that catalytic role with clay minerals during this ISC procedure would be varied with the reaction conditions. In particular, it might lead to even lower combustion efficiency for crude oil during pyrolysis conditions, affecting the propulsive effectiveness of the combustion front and the persistence of this ISC procedure.

Conclusions

This study investigated the catalytic role of diverse clay minerals through DSC experiments for the oxidized and pyrolysis oil thermal reaction process, drawing below conclusions with the results of DSC analysis and kinetic calculations:

- The catalytic role of clay minerals for the thermal transformation with oxidized oil was mainly manifested in that it would shorten LTO reaction temperature region and lower LTO stage peak temperature, facilitating the coke generation and conversion in the FD stage. Moreover, especially in the HTO stage, montmorillonite-containing and illite-containing oxidized oils showed higher peak heat flow, and more heat was generated by combustion.
- The catalytic role of the active sites in montmorillonite enlarged the peak heat flow of pyrolyzed oil at 300 °C and 350 °C during the HTO stage. Nevertheless, the clay minerals had a pronounced retarding role on the crude oil pyrolysis reaction as pyrolysis temperature approached 400 °C. It was hypothesized that the Lewis acid sites within clay minerals affected free radical reactions during crude oil pyrolysis process.
- Clay minerals considerably diminished oxidized oil activation energy during LTO stage, and oxidized oil transition to FD stage from LTO stage was more likely to occur. Furthermore, the FD stage generated more oxidized coke to support the combustion front to continue to move forward and boost the success rate of the ISC procedure. The strong adsorption mechanism and carbon ion mechanism with clay minerals could minimize this activation energy for 300°C and 350°C pyrolyzed oils during LTO and HTO stages. However, the occurrence of thermal transformation reaction was unfavorable by the existence with clay minerals for 400°C pyrolysis oil.

Acknowledgements We appreciate the financial support provided by the National Natural Science Foundation of China (U20B6003). The financial support of a project from China Petroleum and Chemical Corporation (P22174) is also acknowledged.

References

1. Mallory DG, Moore RG, Mehta SA. Ramped temperature oxidation testing and in situ combustion projects. Energy Fuels. 2018;32:8040–56.
2. Amine Ifticene M, Yuan C, Al-Muntaser AA, Onishchenko YV, Emelianov DA, Varfolomeev MA. Behavior and kinetics of the conversion/combustion of oil shale and its components under air condition. Fuel. 2022;324: 124597.
3. Yuan C, Sadikov K, Varfolomeev M, Khaliullin R, Pu W, Al-Muntaser A, et al. Low-temperature combustion behavior of crude oils in porous media under air flow condition for in-situ combustion (ISC) process. Fuel. 2020;259: 116293.
4. Zhao S, Pu W, Varfolomeev MA, Yuan C, Qin S, Wang L, et al. Thermal behavior and kinetics of heavy crude oil during combustion by high pressure differential scanning calorimetry and accelerating rate calorimetry. J Pet Sci Eng. 2019;181: 106225.
5. Kök MV, Varfolomeev MA, Nurgaliev DK. TGA and DSC investigation of different clay mineral effects on the combustion behavior and kinetics of crude oil from Kazan region. Russia J Pet Sci Eng. 2021;200: 108364.
6. Pu W-F, Yuan C-D, Jin F-Y, Wang L, Qian Z, Li Y-B, et al. Low-temperature oxidation and characterization of heavy oil via thermal analysis. Energy Fuels. 2015;29:1151–9.
7. Wu LM, Zhou CH, Keeling J, Tong DS, Yu WH. Towards an understanding of the role of clay minerals in crude oil formation, migration and accumulation. Earth-Sci Rev. 2012;115:373–86.
8. Vossoughi S, Willhite GP, Kritikos WP, Guvenir IM, El Shoubary Y. Automation of an in-situ combustion tube and study of the effect of clay on the in-situ combustion process. Soc Pet Eng J. 1982;22:493–502.
9. Vossoughi S, Willhite G, El Shoubary Y, Bartlett G. Study of the clay effect on crude oil combustion by thermogravimetry and differential scanning calorimetry. J Therm Anal. 1983;27:17–36.

10. Kok MV. Clay concentration and heating rate effect on crude oil combustion by thermogravimetry. Fuel Process Technol. 2012;96:134–9.
11. Kök MV. Effect of clay on crude oil combustion by thermal analysis techniques. J Therm Anal Calorim. 2006;84:361–6.
12. Kok MV, Gundogar AS. Effect of different clay concentrations on crude oil combustion kinetics by thermogravimetry. J Therm Anal Calorim. 2010;99:779–83.
13. Kök MV. Influence of reservoir rock composition on the combustion kinetics of crude oil. J Therm Anal Calorim. 2009;97:397.
14. Ismail NB, Hascakir B. Impact of asphaltenes and clay interaction on in-situ combustion performance. Fuel. 2020;268: 117358.
15. Pope C, Ismail NB, Hascakir B. The role of reservoir fluids and reservoir rock mineralogy on in-situ combustion kinetics. Geoenergy Sci Eng. 2023;224: 211516.
16. Punase AD, Hascakir B. Role of reservoir brine and rock in modulating asphaltene stability: insights from experimental analysis. SPE J. 2023;28:3128–47.
17. Punase A, Prakoso A, Hascakir B. Effect of clay minerals on asphaltene deposition in reservoir rock: insights from experimental investigations. Fuel. 2023;351: 128835.
18. Ranjbar M. Influence of reservoir rock composition on crude oil pyrolysis and combustion. J Anal Appl Pyrolysis. 1993;27:87–95.
19. Bagci S. Effect of clay content on combustion reaction parameters. Energy Sources. 2005;27:579–88.
20. Zheng R, Liao G, You H, Song X, Song Q, Yao Q. Montmorillonite-catalyzed thermal conversion of low-asphaltene heavy oil and its main components. J Pet Sci Eng. 2020;187: 106743.
21. Zheng R, Pan J, Cai G, Liang J, Liu D, Song Q, et al. Effects of clay minerals on the low-temperature oxidation of heavy oil. Fuel. 2019;254: 115597.
22. Li Y-B, Lin X, Luo C, Hu Z-M, Jia H-F, Chen J-T, et al. A comprehensive investigation of the influence of clay minerals on oxidized and pyrolyzed cokes in in situ combustion for heavy oil reservoirs. Fuel. 2021;302: 121168.
23. Li Y-B, Zhang S-X, Luo C, Zhao S, Wei B, Pu W-F. An experimental investigation in the formation damage mechanism of deposited coke in in-situ combustion process using nuclear magnetic resonance. Fuel. 2022;313: 122703.
24. Luo C, Liu H, Li X, Dong X, Zhang Y, Wang H. Effects of different clay minerals on thermal conversion of oxidized and pyrolyzed oils during in situ combustion. J Therm Anal Calorim. 2023;148:12629–37.
25. Li Y-B, Luo C, Lin X, Li K, Xiao Z-R, Wang Z-Q, et al. Characteristics and properties of coke formed by low-temperature oxidation and thermal pyrolysis during in situ combustion. Ind Eng Chem Res. 2020;59:2171–80.
26. Pu W, Pang S, Jia H. Using DSC/TG/DTA techniques to re-evaluate the effect of clays on crude oil oxidation kinetics. J Pet Sci Eng. 2015;134:123–30.
27. Yuan C, Emelianov DA, Varfolomeev MA. Oxidation behavior and kinetics of light, medium, and heavy crude oils characterized by thermogravimetry coupled with fourier transform infrared spectroscopy. Energy Fuels. 2018;32:5571–80.
28. Zhao S, Xu C, Pu W, Varfolomeev MA, Zhou Y, Yuan C, et al. Oxidation characteristics and kinetics of shale oil using high-pressure differential scanning calorimetry. Energy Fuels. 2021;35:18726–32.
29. Saitova A, Strokin S, Ancheyta J. Evaluation and comparison of thermodynamic and kinetic parameters for oxidation and pyrolysis of Yarega heavy crude oil asphaltenes. Fuel. 2021;297: 120703.
30. Zhang X, Wang J, Wang L, Li Z, Wang R, Li H, et al. Effects of kaolinite and its thermal transformation on oxidation of heavy oil. Appl Clay Sci. 2022;223: 106507.
31. Kök MV. Effect of pressure and particle size on the thermal cracking of light crude oils in sandstone matrix. J Therm Anal Calorim. 2009;97:403–7.
32. Yuan C, Emelianov DA, Varfolomeev MA, Rodionov NO, Suwaid MA, Vakhitov IR. Mechanistic and kinetic insight into catalytic oxidation process of heavy oil in in-situ combustion process using copper (II) stearate as oil soluble catalyst. Fuel. 2021;284: 118981.
33. Chen Y, Yin H, He D, Gong H, Liu Z, Liu Y, et al. Low temperature oxidized coke of the ultra-heavy oil during in-situ combustion process: structural characterization and evolution elucidation. Fuel. 2022;313: 122676.
34. Zhao S, Pu W, Peng X, Zhang J, Ren H. Low-temperature oxidation of heavy crude oil characterized by TG, DSC, GC-MS, and negative ion ESI FT-ICR MS. Energy. 2021;214: 119004.
35. Yuan C, Varfolomeev MA, Emelianov DA, Suwaid MA, Khachatrian AA, Starshinova VL, et al. Copper stearate as a catalyst for improving the oxidation performance of heavy oil in in-situ combustion process. Appl Catal Gen. 2018;564:79–89.
36. Ariskina KA, Yuan C, Abaas M, Emelianov DA, Rodionov N, Varfolomeev MA. Catalytic effect of clay rocks as natural catalysts on the combustion of heavy oil. Appl Clay Sci. 2020;193: 105662.
37. Zheng R, Liu D, Tang J, Song Q, Yao Q. Analysis of montmorillonite affecting coke formation during the thermal conversion of heavy oil. Fuel. 2021;288: 119687.
38. Sanyal S, Bhui UK, Balaga D, Kumar SS. Interaction study of montmorillonite-crude oil-brine: molecular-level implications on enhanced oil recovery during low saline water flooding from hydrocarbon reservoirs. Fuel. 2019;254: 115725.
39. Sudibyo H, Cabrera DV, Widyaparaga A, Budhijanto B, Celis C, Labatut R. Reactivity and stability of natural clay minerals with various phyllosilicate structures as catalysts for hydrothermal liquefaction of wet biomass waste. Ind Eng Chem Res. 2023;62:12513–29.
40. Rawat A, Dhakla S, Maity SK, Lama P. Mechanistic insight into the coke formation tendency during upgradation of crude oil in slurry phase batch reactor using MoS_2 and its various oil soluble catalysts. Fuel. 2024;359: 130433.
41. Yang Y, Liang X, Li X. Investigation of clay-oil interfacial interactions in petroleum-contaminated soil: effect of crude oil composition. J Mol Liq. 2023;380: 121702.
42. Zheng R, Pan J, Chen L, Tang J, Liu D, Song Q, et al. Catalytic effects of montmorillonite on coke formation during thermal conversion of heavy oil. Energy Fuels. 2018;32:6737–45.
43. Xiao Q, Sun Y, Zhang Y. The role of reservoir mediums in natural oil cracking: preliminary experimental results in a confined system. Chin Sci Bull. 2010;55:3787–93.
44. Wang L, Wang T, Bai Z, Yuan C, Song W, Chen Y, et al. Thermo-oxidative behavior and kinetics analysis of light and heavy oils based on TG, DSC, and FTIR. Geoenergy Sci Eng. 2023;223: 211525.
45. Zhao S, Pu W, Chen Q, Yuan C, Varfolomeev MA. Propagation of combustion front within fractured shale and its influence on shale structure and crude oil properties: an experimental study. SPE J. 2024;29: 238998.
46. Zhang X, Ren D, Yao Y. A new family Jubisentidae fam. nov. (Hemiptera: Fulgoromorpha: Fulgoroidea) from the mid-Cretaceous Burmese amber. Cretac Res. 2019;94:1–7.
47. Kemp SJ. The clay minerals group (CMG): 1947–2022. Clay Miner. 2023;58:38–56.

48. Torres-Luna JA, Carriazo JG. Porous aluminosilicic solids obtained by thermal-acid modification of a commercial kaolinite-type natural clay. Solid State Sci. 2019;88:29–35.